Quasielectrostatic instabilities excited by energetic oxygen ions in the ring current region

S. V. Singh,[a] A. P. Kakad, and G. S. Lakhina
Indian Institute of Geomagnetism, Plot No. 5, Sector 18, New Panvel (West), Navi Mumbai 410218, India

(Received 30 March 2004; accepted 12 October 2004; published online 14 December 2004)

Quasielectrostatic instabilities driven by anisotropic oxygen ions are investigated during storms/substorms in three-component ring current plasma consisting of electrons, protons, and energetic oxygen ions having loss-cone distribution. The response of the electrons is fully electromagnetic and that of the protons and oxygen ions is electrostatic. The electrons, protons, and oxygen ions are treated as magnetized. Obliquely propagating modes with frequencies near the harmonics of the oxygen ion cyclotron frequency are found to become unstable due to pressure anisotropy of the energetic oxygen ions. The results are applied to storm-time ring-current region parameters. The loss of energetic particles resulting from wave-particle interaction may provide an alternate mechanism, complimentary to and independent of the charge exchange process for the ring-current decay.
 [DOI: 10.1063/1.1828465]

I. INTRODUCTION

Low-frequency waves with frequencies from a few hertz to a few kilohertz have been observed in the various regions of the Earth's magnetosphere by several spacecrafts, e.g., OGO 3, IMP 6, S3-3, GEOS 1 and 2, Viking, etc.[1–7] These waves can be generated by energetic proton or heavier ion distributions. In the ring-current region a quasielectrostatic instability can be excited by loss-cone distributions of protons and oxygen ions.[8–13]

Energetic oxygen ions with hundreds of keV energies have been observed in various regions of the Earth's magnetosphere.[14,15] Oxygen ions (O^+) of ionospheric origin are important constituents of the ring current. The energy content of geomagnetically trapped particles increases during the main phase of a storm, and the fractional concentration of oxygen ions is also enhanced.[16,17] Fractional concentration of these oxygen ions can reach a value in excess of hydrogen ions for the largest magnetic storms. The presence of oxygen ions during storms can affect the excitation of low-frequency instabilities such as electromagnetic ion cyclotron (EMIC) instability. Thorne and Horne[18] showed that during geomagnetic storms when the oxygen ion content is significantly enhanced, the absorption of EMIC waves become efficient and may lead to the acceleration of O^+ ions of ionospheric origin to ring-current energies. During modest storms, strong EMIC excitation can occur in the frequency band above the oxygen gyrofrequency due to cyclotron resonance with anisotropic ring-current H^+ ions. The energy of the excited wave is efficiently converted into the perpendicular heating of the O^+ ions thus making them more anisotropic during the main phase of the magnetic storm.

We study the obliquely propagating quasielectrostatic waves generated by anisotropic oxygen ions in the ring-current region during the main phase of magnetic storms. The particle distributions in the ring current are generally non-Maxwellian. The physics is expected to be different and analysis much more complicated, when protons and electrons are described by the Dory–Guest–Harris (DGH) distributions.[8,19] As a first order approximation, we consider electrons and protons to be Maxwellian, and energetic oxygen ions to have a loss-cone-type distribution modeled by DGH-type distribution. Further, the response of the electrons is fully electromagnetic, while that of protons and oxygen ions is considered as electrostatic. In the following section a theoretical model and numerical results are presented. Results are summarized and discussed in the last section.

II. THEORETICAL ANALYSIS

We consider a three-component ring-current plasma consisting of Maxwellian distributed electrons with density N_e and temperature T_e; protons with density N_p and temperature T_p; and DGH-type distributed oxygen ions with density N_o and parallel (perpendicular) temperature $T_{\|o}(T_{\perp o})$ given by

$$f_o = \frac{N_o}{\pi^{3/2}} \frac{1}{J!\,\alpha_o^3} \left(\frac{v_\perp}{\alpha_o}\right)^{2J} \exp\left[-\frac{v_\perp^2 + v_\|^2}{\alpha_o^2}\right], \tag{1}$$

where the loss-cone index $J=(T_{\perp o}/T_{\|o}-1)$, which defines the temperature anisotropy, and $\alpha_o=\sqrt{2T_{\|o}/m_o}$ is the parallel thermal velocity of the oxygen ions. All the three components are treated as magnetized, i.e., $\omega < \omega_{cp}, \omega_{co} \ll \omega_{ce}$. The response of the electrons is fully electromagnetic, i.e., $\omega_{pe}^2/c^2k^2 \gg 1$, while protons and oxygen ions are considered to be electrostatic, i.e., $\omega_{pp}^2/c^2k^2 \ll 1$ and $\omega_{po}^2/c^2k^2 \ll 1$. Thus, under the above assumptions, a dispersion relation for the low-frequency waves propagating obliquely to the magnetic field $\mathbf{B}_o \| \mathbf{z}$ can be obtained by solving the linearized Vlasov equation along with Maxwell's equations and is written as[8,20,21]

[a]Author to whom correspondence should be addressed. Electronic mail: satyavir@iigs.iigm.res.in

$$1+\frac{\omega_{pe}^2}{\omega_{ce}^2}\left[\frac{1-I_0(\lambda_e)e^{-\lambda_e}}{\lambda_e}\right]+\frac{\omega_{pe}^2}{\omega_{ce}^2}\frac{\omega_{pe}^2}{c^2k^2}\left[\frac{\{[I_0(\lambda_e)-I_1(\lambda_e)]e^{-\lambda_e}\}^2}{1+\beta_e[I_0(\lambda_e)-I_1(\lambda_e)]e^{-\lambda_e}}\right]-\frac{k_\parallel^2}{k_\perp^2}\frac{\omega_{pe}^2}{\omega^2}\frac{I_0(\lambda_e)e^{-\lambda_e}}{1+\frac{\omega_{pe}^2}{c^2k^2}I_0(\lambda_e)e^{-\lambda_e}}-\sum_{n=1}^{\infty}\frac{4n^2\omega_{pp}^2\omega_{cp}^2}{k_\perp^2\alpha_p^2(\omega^2-n^2\omega_{cp}^2)}I_n(\lambda_p)e^{-\lambda_p}+\sum_{l=-\infty}^{\infty}\frac{2\omega_{po}^2}{k^2\alpha_o^{2J+4}}\frac{(-1)^J}{J!}\left\{\left[1+\frac{\omega\sqrt{\mu}}{k_\parallel}Z(\xi)\right]\frac{d^JR_l}{d\mu^J}+\frac{lJ\omega_{co}}{k_\parallel\sqrt{\mu}}Z(\xi)\frac{d^{J-1}R_l}{d\mu^{J-1}}\right\}=0, \tag{2}$$

where, in the following, the subscript $s=e,p,o$ refers to electrons, protons, and oxygen ions, respectively; $Z(\xi)$ is the plasma dispersion function with respect to its argument $\xi=(\omega-l\omega_{co})\sqrt{\mu}/k_\parallel$; and $\omega_{ps}=(4\pi N_se^2/m_s)^{1/2}$ and $\omega_{cs}=eB_o/cm_s$, respectively, are the plasma and cyclotron frequencies of the species s; N_s and m_s are the density and mass of the species s; k is the wave number; c is the velocity of light, $\lambda_{e,p}=k_\perp^2\alpha_{e,p}^2/2\omega_{ce,p}^2$, $\mu^{-1}=\alpha_o^2=2T_{\parallel o}/m_o$ and $R_l=1/\mu I_l(\lambda_o)e^{-\lambda_o}$; $I_l(\lambda_o)$ is the modified Bessel function of order l and argument $\lambda_o=k_\perp^2\alpha_o^2/2\omega_{co}^2$. We assume protons to be cold as a first order approximation and retain $n=1$ terms for them as the frequency of the wave is much less than the proton cyclotron frequency, i.e., $\omega\ll\omega_{cp}$ and the contribution from the higher order terms will be very small. Expanding the plasma dispersion function for oxygen ions in the limit $\xi\ll1$ for $\omega\simeq m\omega_{co}$ and substituting for $\omega=\omega_r+i\gamma$, $\gamma\ll\omega_r$ in Eq. (2), we obtain an expression for real frequency ω_r and growth rate γ given by

$$\omega_r=\pm\sqrt{Q/P}, \tag{3}$$

$$\gamma\simeq-\frac{\sqrt{\pi}}{Q}\frac{\omega_r^3\omega_{po}^2}{k_\parallel k^2\alpha_o^{2J+5}}\frac{(-1)^J}{J!}\left[\omega_r\frac{d^JR_m}{d\mu^J}+\frac{mJ\omega_{co}}{\mu}\frac{d^{J-1}R_m}{d\mu^{J-1}}\right], \tag{4}$$

where

$$P=1+\frac{\omega_{pe}^2}{\omega_{ce}^2}\left[\frac{1-I_0(\lambda_e)e^{-\lambda_e}}{\lambda_e}\right]+\frac{\omega_{pe}^2}{\omega_{ce}^2}\frac{\omega_{pe}^2}{c^2k^2}\left[\frac{\{[I_0(\lambda_e)-I_1(\lambda_e)]e^{-\lambda_e}\}^2}{1+\beta_e\{I_0(\lambda_e)-I_1(\lambda_e)\}e^{-\lambda_e}}\right]+\frac{\omega_{pp}^2}{\omega_{cp}^2}+\frac{(-1)^J}{J!}\frac{2\omega_{po}^2}{k^2\alpha_o^{2J+4}}\frac{d^JR_m}{d\mu^J}, \tag{5}$$

$$Q=\frac{k_\parallel^2}{k_\perp^2}\frac{\omega_{pe}^2I_0(\lambda_e)e^{-\lambda_e}}{1+\frac{\omega_{pe}^2}{c^2k^2}I_0(\lambda_e)e^{-\lambda_e}}. \tag{6}$$

In writing Eqs. (3) and (4) we have retained the contributions from the $l=m$ term only for the oxygen ions. It can be seen from the growth rate expression (4) that for $J=0$, i.e., when perpendicular and parallel temperatures of oxygen ions are equal and hence, there is no anisotropy, the growth rate is negative and waves are damped. It is expected as in this case there is no source of free energy to drive the waves unstable. The growth rate for $J=1$ and $m=1$ is given by

$$\gamma=\frac{\sqrt{\pi}}{Q}\frac{\omega_r^3\omega_{po}^2}{k_\parallel k^2\alpha_o^3}e^{-\lambda_0}[\omega_r\lambda_o(I_1-I_0)+\omega_{co}I_1] \tag{7}$$

and for $J=2$, $m=1$ the growth rate is given by

$$\gamma=-\frac{\sqrt{\pi}}{2Q}\frac{\omega_r^3\omega_{po}^2}{k_\parallel k^2\alpha_o^3}\lambda_oe^{-\lambda_0}\{\omega_r[(2\lambda_o-2)I_1+(3-2\lambda_o)I_0]+2\omega_{co}(I_1-I_0)\} \tag{8}$$

and similarly for $J=3$, $m=1$ the growth rate is given by

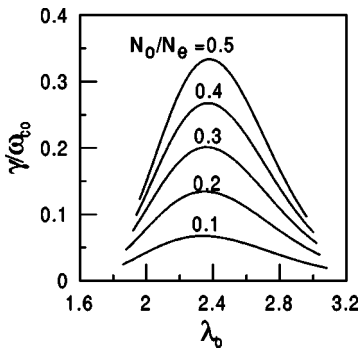

FIG. 1. The variation of normalized growth rate γ/ω_{co} with $\lambda_o=k_\perp^2\alpha_o^2/2\omega_{co}^2$ for various values of the fractional oxygen ion density N_o/N_e as shown on the curves. The other parameters are $J=1$, $m=1$, $k_\parallel/k=0.09$, $T_{\parallel o}/T_e=20$, $\omega_{pe}/\omega_{ce}=2$, $N_e=10$ cm^{-3}, and $B_o=5\times10^{-3}$ G.

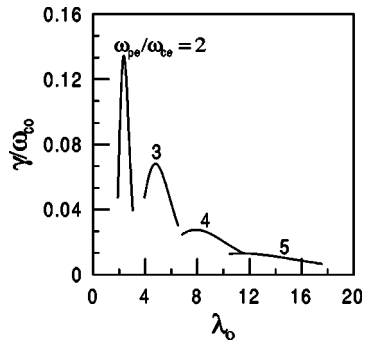

FIG. 2. The variation of normalized growth rate with λ_o for various values of ω_{pe}/ω_{ce} as shown on the respective curves for $N_o/N_e=0.2$ (which is used in all subsequent figures). The other parameters are the same as in Fig. 1.

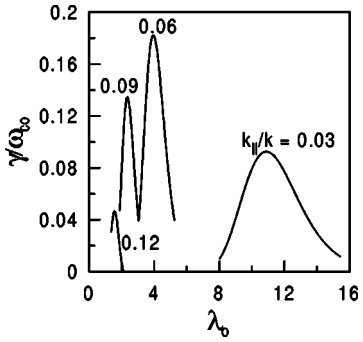

FIG. 3. The effect of $k_\parallel/k$ (propagation angle) on the growth rate N_o/N_e =0.2. The other parameters are the same as in Fig. 1.

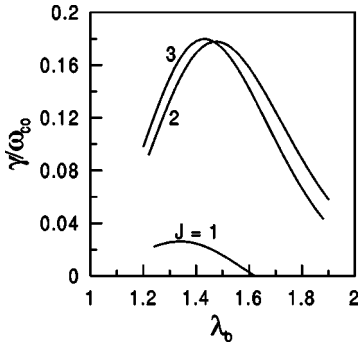

FIG. 5. Comparison of growth rates for $J=1$, 2, and 3 for $N_o/N_e=0.2$ and $k_\parallel/k=0.13$. The other parameters are the same as in Fig. 1.

$$\gamma = \frac{\sqrt{\pi}}{6Q}\frac{\omega_r^3\omega_{po}^2}{k_\parallel k^2\alpha_o^3}\lambda_o e^{-\lambda_0}\{\omega_r[(4\lambda_o^2 - 13\lambda_0 + 6)I_1 - (4\lambda_0^2 - 15\lambda_0 + 12)I_0] + \omega_{co}[(6\lambda_0 - 6)I_1 + (9 - 6\lambda_o)I_0)]\}. \tag{9}$$

Real frequency and growth rate are obtained numerically by solving Eqs. (3) and (4), respectively, for different values of J and m by using MATHEMATICA. For our numerical calculations, the chosen parameters for the $J=1$, $m=1$ case are $k_\parallel/k=0.09$, $T_{\parallel o}/T_e=20$, $\omega_{pe}/\omega_{ce}=2$, $T_e=1$ keV, $N_e=10$ cm^{-3}, and $B_o=5\times10^{-3}$ G, which are representative of storm-time ring-current region and have been used for all the calculations presented in this paper.

Figure 1 shows the variation of normalized growth rate γ/ω_{co} with $\lambda_o=k_\perp^2\alpha_o^2/2\omega_{co}^2$ for various values of the fractional oxygen ion density N_o/N_e as shown on the curves. Here, λ_o is effectively the square of the transverse wave number normalized with respect to oxygen ion Larmor radius which is defined as ratio of parallel thermal velocity to cyclotron frequency of oxygen ions. It can be seen from the figure that the growth rate increases with the increase in the fractional density of the oxygen ions. It is pointed out here that all the growth rate curves in Figs. 1–4 have been plotted for the normalized real frequency $\omega_r/\omega_{co}\simeq(0.8-1.2)$.

Figure 2 shows the variation of normalized growth rate with λ_o for various values of ω_{pe}/ω_{ce} as shown by the respective curves for $N_o/N_e=0.2$ (which is used in all subsequent figures). The growth rate is higher for the smaller ω_{pe}/ω_{ce} values, i.e., the smaller the magnetic field, the smaller is the growth rate for the fixed oxygen ion concentration. However, the range of excited wave numbers increases with the increase in ω_{pe}/ω_{ce} values.

The effect of $k_\parallel/k$ (propagation angle) on the growth rate is shown in Fig. 3. The growth rate first increases with the increase in $k_\parallel/k$ values, reaches a maximum, and then decreases. Also the range of unstable wave numbers decreases with the increase of $k_\parallel/k$.

In Fig. 4, the variation of normalized growth rate is shown for various values of parallel oxygen ion to electron temperature ratio $(T_{\parallel o}/T_e)$. The growth rate of the low-frequency waves first increases with the increase in $T_{\parallel o}/T_e$ values and then decreases after reaching a maximum value. However, the range of unstable wave numbers increases with increase in $(T_{\parallel o}/T_e)$.

In Fig. 5, we show a comparison of the growth rates for $J=1$, 2, and 3 values of the temperature anisotropies, for $T_{\parallel o}/T_e=20$, $N_o/N_e=0.2$, and $k_\parallel/k=0.13$, the other parameters are same as in Fig. 1. It is interesting to note that the growth rate increases with an increase in anisotropy.

We have also carried out numerical calculations for real frequencies and growth rates of different harmonics (m =1–4) of the oxygen cyclotron frequencies for $J=1$, by solving the Eqs. (3) and (4), respectively. The results are shown in the form of graphs in Fig. 6 for $N_o/N_e=0.2$. The other parameters are same as for Fig. 1. Real frequencies (shown on right-hand side scale) and growth rates (shown on left-

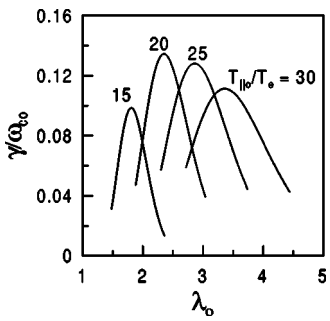

FIG. 4. The variation of normalized growth rate is shown for the various values temperature ratio $(T_{\parallel o}/T_e)$ for $N_o/N_e=0.2$. The other parameters are the same as in Fig. 1.

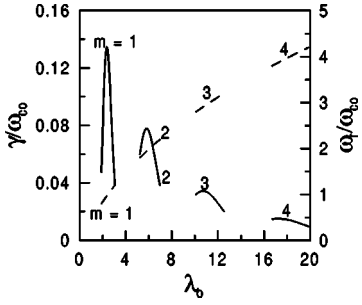

FIG. 6. Comparison of growth rates [represented by solid lines (—) and scale on left-hand side] of different harmonics ($m=1-4$) of the oxygen cyclotron frequencies for $J=1$, $N_o/N_e=0.2$. The other parameters are the same as for Fig. 1. The corresponding real frequencies are represented by dashed lines (----) and scale on right-hand side.

hand side scale) are represented by dashed lines (----) and solid lines (—), respectively. It can be seen from the figure that the growth rate decreases for higher harmonics but the range of wave numbers increases. The curves in Fig. 6 are restricted to $\omega_r=(0.8-1.2)\omega_{co}$ for $m=1$, $\omega_r=(1.8-2.2)\omega_{co}$ for $m=2$, $\omega_r=(2.8-3.2)\omega_{co}$ for $m=3$, and $\omega_r=(3.8-4.2)\omega_{co}$ for $m=4$, respectively.

III. CONCLUSION

We have carried out numerical calculations of the growth rate for $m\simeq 1$, i.e., $\omega_r\simeq\omega_{co}$ for three different values of the anisotropic index J for the storm-time ring-current parameters. For $T_{\|o}/T_e=20$ and $J=1$, 2, and 3, the growth rate $\gamma\approx(10-13)$ mHz, $(29-89)$ mHz, and $(29-90)$ mHz, respectively, and the growth rate increases with increase in anisotropy. The real frequency and perpendicular wavelengths of these low-frequency waves for the above J values are found to be in the range $\omega_r\approx(400-600)$ mHz and $\lambda_\perp\approx(480-610)$ km, respectively.

Now, we estimate the saturation electric field amplitude of the waves by equating the linear wave growth rate with the trapping frequency $[\omega_t=(ekE_s/m_o)^{1/2}]$ of the oxygen ions.[8] Thus, here we assume that the modes are stabilized by the trapping of O^+ ions by the waves when their amplitude becomes large and the saturation electric field E_s for the low-frequency waves can then, be given by

$$E_s\simeq\frac{m_o}{e}\frac{\gamma^2}{k}. \tag{10}$$

In order to estimate the diffusion time for an oxygen ion to reach the loss cone, we construct a diffusion coefficient D given by

$$D=(\Delta v_\perp)^2/2\Delta t, \tag{11}$$

where $\Delta v_\perp=eE_s\Delta t/m_o$ and Δt is the wave-particle correlation time. Since $\gamma\sim(ekE_s/m_o)^{1/2}$, and assuming $\Delta t\approx\gamma^{-1}$, D is given by

$$D\simeq\frac{\gamma^3}{2k^2}. \tag{12}$$

The saturation electric fields for $T_{\|o}/T_e=20$ and $J=1$, 2, and 3 as calculated from (10) are $\simeq(60-100)$ μV/m, $(0.4-4.5)$ mV/m, and $(0.4-4.7)$ mV/m, respectively, and the corresponding diffusion coefficients as calculated from (12) are found to be of the order of $(1-20)\times10^9$ cm^2/s^3, $(2-70)\times10^{11}$ cm^2/s^3, and $(2-72)\times10^{11}$ cm^2/s^3, respectively. The typical time during which an oxygen ion can diffuse into loss cone with a velocity α_o is in the range (10^2-10^6) s.

It is shown here that low-frequency quasielectrostatic waves can be excited by anisotropic oxygen ions near the harmonics of the oxygen ion cyclotron frequency and have large growth rate for nearly perpendicular propagation. The growth rate is found to increase with an increase in the fractional oxygen ion concentration. Growth time of these waves is a few tens of seconds to a few minutes, whereas the geomagnetic storm main phase lasts for several hours. The low-frequency waves studied here may scatter ring-current particles into the loss cone leading to their precipitation in the ionosphere and consequently depleting the ring current of these particles. Several authors[22–25] have proposed charge exchange of ring current ions with neutral hydrogen as a main mechanism for the ring current decay. It is also shown that the scattering of protons by electromagnetic ion cyclotron waves can contribute to ring-current decay.[26] Here, we have shown that the scattering of ring-current particles by the low-frequency quasielectrostatic waves could also lead to the ring-current decay. This mechanism would be complementary to the charge exchange.

In our model, we have considered DGH-type distribution for oxygen ions and Maxwellian distribution for electrons and protons. One can consider DGH-type distribution for protons and electrons also. However, the physics is expected to be different, and the analysis much more complicated, which is beyond the scope of this paper. We are carrying out the analysis by including DGH-type protons and extending the present work, which will be presented in a future publication.

[1] C. T. Russel, R. E. Holzer, and E. J. Smith, J. Geophys. Res. **75**, 755 (1970).
[2] R. R. Anderson and D. A. Gurnett, J. Geophys. Res. **78**, 4756 (1973).
[3] D. A. Gurnett, J. Geophys. Res. **81**, 2765 (1976).
[4] D. A. Gurnett and L. A. Frank, J. Geophys. Res. **82**, 1031 (1977).
[5] D. A. Gurnett and L. A. Frank, J. Geophys. Res. **83**, 1447 (1978).
[6] S. Perraut, A. Roux, P. Robert, R. Gendrin, J. A. Sauvaud, J. M. Bosqued, G. Kremser, and A. Korth, J. Geophys. Res. **87**, 6219 (1982).
[7] H. Laakso, H. Junginger, A. Roux, R. Schmidt, and C. de Villedary, J. Geophys. Res. **95**, 10609 (1990).
[8] F. V. Coroniti, R. W. Fredricks, and R. White, J. Geophys. Res. **77**, 6243 (1972).
[9] W. Bernstein, B. Hultqvist, and H. Borg, Planet. Space Sci. **22**, 767 (1974).
[10] G. S. Lakhina, Planet. Space Sci. **24**, 609 (1976).
[11] K. G. Bhatia and G. S. Lakhina, Astrophys. Space Sci. **68**, 175 (1980).
[12] S. V. Singh, A. P. Kakad, R. V. Reddy, and G. S. Lakhina, J. Plasma Phys. **70**, 613 (2004).
[13] G. S. Lakhina and S. Singh, in *Geophysical Monograph Series Disturbances in Geospace: The Storm-Substorm Relationship*, edited by A. Surjalal Sharma, Y. Kamide, and G. S. Lakhina (American Geophysical Union, Washington, DC, 2003), Vol. 142, p. 131.
[14] M. Nose, A. T. Y. Lui, S. Ohtani, B. H. Mauk, R. W. McEntire, D. J. Williams, T. Mukai, and K. Yumoto, J. Geophys. Res. **105**, 7669 (2000).
[15] J. Chen and T. A. Fritz, Geophys. Res. Lett. **28**, 1459 (2001).
[16] G. Gloeckler and D. C. Hamilton, Phys. Scr. **T18**, 73 (1987).
[17] D. C. Hamilton, G. Gloeckler, F. M. Ipovitch, W. Studenmann, B. Wilken, and G. Kremser, J. Geophys. Res. **93**, 14343 (1988).
[18] R. M. Thorne and R. B. Horne, J. Geophys. Res. **99**, 17275 (1994).
[19] R. A. Dory, G. E. Guest and E. G. Harris, Phys. Rev. Lett. **14**, 131 (1965).
[20] R. C. Davidson, N. T. Gladd, C. S. Wu, and J. D. Huba, Phys. Fluids **20**, 301 (1977).
[21] K. G. Bhatia and G. S. Lakhina, Planet. Space Sci. **25**, 833 (1977).
[22] M.-C. Fok, T. E. Moore, J. U. Kozyra, G. C. Ho, and D. C. Hamilton, J. Geophys. Res. **100**, 9619 (1995).
[23] M. W. Chen, M. Schulz, and L. R. Lyons, in *Geophysical Monograph Series Magnetic Storms*, edited by B. T. Tsurutani, W. D. Gonzalez, Y. Kamide, and J. K. Arballo (American Geophysical Union, Washington, DC, 1997), Vol. 98, p. 173.
[24] I. A. Daglis, R. M. Thorne, W. Baumjohann, and S. Orsini, Rev. Geophys. **37**, 407 (1999).
[25] Y. Ebihara and M. Ejiri, Adv. Polar Upper Atmos. Res. **13**, 1 (1999).
[26] J. U. Kozyra, V. K. Jordanova, R. B. Horne, and R. M. Thorne, in *Geophysical Monograph Series Magnetic Storms*, edited by B. T. Tsurutani, W. D. Gonzalez, Y. Kamide, and J. K. Arballo (American Geophysical Union, Washington, DC, 1997), Vol. 98, p. 107.